Cost-effective fire protection of chemical plants against domino effects

Khakzad, N.; Landucci, Gabriele; Cozzani, Valerio; Reniers, Genserik; Pasman, HJ

DOI
10.1016/j.ress.2017.09.007

Publication date
2018

Document Version
Accepted author manuscript

Published in
Reliability Engineering & System Safety

Cost-effective fire protection of chemical plants against domino effects

Nima Khakzad , Gabriele Landucci , Valerio Cozzani , Genserik Reniers , Hans Pasman

PII: S0951-8320(16)30168-5
DOI: 10.1016/j.ress.2017.09.007
Reference: RESS 5945

To appear in: *Reliability Engineering and System Safety*

Received date: 21 June 2016
Revised date: 31 July 2017
Accepted date: 22 September 2017

Please cite this article as: Nima Khakzad , Gabriele Landucci , Valerio Cozzani , Genserik Reniers , Hans Pasman , Cost-effective fire protection of chemical plants against domino effects, *Reliability Engineering and System Safety* (2017), doi: 10.1016/j.ress.2017.09.007

Highlights

- Effect of fire protection systems on domino scenarios has been modeled using a Bayesian network technique.
- Optimal allocation of fire protection systems has been performed by extending the Bayesian network to an influence diagram.

Cost-effective fire protection of chemical plants against domino effects

Nima Khakzad[1,*], Gabriele Landucci[2], Valerio Cozzani[3], Genserik Reniers[1], Hans Pasman[4]

1. Safety and Security Science Group, Delft University of Technology, The Netherlands

2. Dipartimento di Ingegneria Civile e Industriale, Università di Pisa, Italy

3. LISES - Dipartimento di Ingegneria Civile, Chimica, Ambientale e dei Materiali, Università di Bologna, Italy

4. Mary Kay O'Connor Process Safety Center, Texas A&M University, United States.

* Corresponding author:

Nima Khakzad

Email: n.khakzadrostami@tudelft.nl

Office: +31 15 27 84709

Fax: +31 15 27 87155

Abstract

The propagation of fire-induced domino effects in chemical plants largely depends on the feature of the primary fire scenario, on separation distances between the units, and on the presence of fire protection barriers. Engineering (add-on) passive and active safety barriers are widely employed to prevent or delay the initiation or propagation of domino effects. In the present study, a methodology has been developed based on Bayesian network to account for the impact of engineering safety barriers on the propagation of fire domino scenarios. The Bayesian network has been extended to a limited memory influence diagram in order to identify a cost-effective allocation of additional safety barriers needed to further mitigate the fire propagation. The application of the methodology has been demonstrated using a chemical tank farm. The comparison of the results obtained from the limited memory influence diagram with the results obtained from a graph theoretic approach developed in a previous work illustrates the reliability of the developed methodology in cost-effective fire protection of chemical plants.

Keywords: Domino effect; Fire protection systems; Bayesian network; Limited memory influence diagram

1. Introduction

Over the past decades, domino effects (also known as escalation of accidents) have been responsible of several catastrophic accidents in chemical and process industry (Khan and Abbasi, 1999; Darbra and Casal, 2010). Some examples are the LPG (liquefied petroleum gas) explosions in a tank farm in Mexico in 1984 (San Juanico disaster) (Arturson, 1987), fires and explosions at the Hertfordshire Oil Storage Terminal in UK in 2005 (Buncefield fire) (BBC, 2010), and more recently, the Caribbean Petroleum Refining tank explosions and fires in Puerto Rico in 2009 (CSB, 2015). Due to their catastrophic consequences, domino effects since several years have been recognized in technical standards and legislation concerned with the control of major accident hazards, such as in the case of the European SEVESO directive (2012).

Although there have been many attempts to model and assess the risk of domino effects (Bagster and Pitblado, 1991; Gledhill and Lines, 1998; Khan and Abbasi, 1998; Vilchez et al., 2001; Reniers et al., 2005; Cozzani et al., 2005; Landucci et al., 2009; Nguyen et al., 2009; Abdolhamidzadeh et al., 2010; Khakzad et al., 2013), less emphasis has been given to the key role of safety barriers in prevention and mitigation of domino effects. Although chemical and process plants are obliged to consider fire protection measures as an integral part of plants' safety management (NFPA, 2009), only a few of previous studies have taken into account the influence of such safety measures on the escalation probabilities and the propagation of domino effect scenarios (Landucci et al., 2015). Inherently safer design techniques such as internal safety distances among hazardous units can also play an important role in preventing or reducing the likelihood of domino effects (Cozzani et al., 2009; Bernechea and Arnaldos, 2014); for existing industrial facilities, however, implementing the inherently safer techniques or macro-layout modification is not easily practicable due to financial and operational constraints.

Aside from inherently safer measures, engineering active and passive safety barriers – also known as add-on safety barriers – such as sprinkler and deluge systems (active measures) as well as fireproofing of units (passive measure) are of utmost importance in the prevention, control, and mitigation of domino effects (Landucci et al., 2015). Several studies have been carried out to develop risk-informed approaches for cost-benefit or cost-effective fireproofing of chemical plants subject to domino effects (Di Padova et al., 2011; Tugnoli et al., 2012). However, in none of the previous works, have the performance of the safety measures been taken into account, leading to a conservative estimate of escalation probabilities and risk. Landucci et al. (2015) introduced a methodology based on event tree to investigate the impact of add-on safety barriers on the prevention and control of domino effects, considering both the availability and effectiveness (hereafter referred altogether as the performance) of the safety barriers.

The present study aims to develop a methodology based on Bayesian network (Pearl, 1988; Jensen and Nielsen, 2007) to account for the impact of add-on safety barriers on the escalation of domino scenarios. The developed Bayesian network (BN) will be extended to a limited memory influence diagram (LIMID) in order to conduct an innovative multi-criteria decision analysis for cost-effective risk management of domino effects. A brief description of BN and LIMID is provided in Section 2. The characteristics of active and passive fire safety barriers and their implementation in the BN are discussed in Section 3. In Section 4, the application of the methodology is demonstrated using a chemical storage plant. Conclusions of this study are presented in Section 5.

2. Probabilistic reasoning

2.1. Bayesian network

Bayesian networks (Pearl, 1988; Jensen and Nielsen, 2007) represent all conditional dependencies (and independencies) among a system's variables by means of joint probability distributions. BNs are acyclic directed graphs in which the systems' random variables (components) are represented by nodes (conventionally, elliptical) while the direct probabilistic dependencies among the nodes are represented by directed arcs. The nodes with arcs directed from them are called parents while the ones with arcs directed into them are called children. The nodes with no parents are also called root nodes, whereas the nodes with no children are known as leaf nodes (Figure 1(a)).

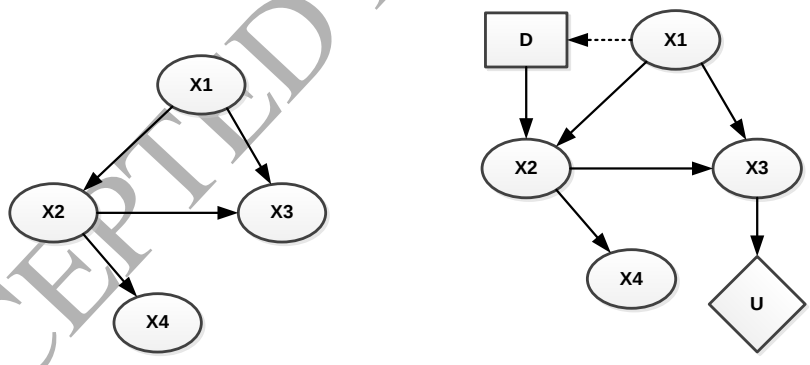

(a) (b)

Figure 1. (a) A Bayesian network consisting of four chance nodes. (b) A limited memory influence diagram by adding decision node D and a utility node U to the Bayesian network.

Satisfying the so-called Markov condition, which states that a node (e.g., X_4 in Figure 1(a)) is independent of its non-descendants (e.g., X_1 and X_3 in Figure 1(a)) given its parents (e.g., X_2 in Figure 1(a)), a BN factorizes a joint probability distribution of its random variables (nodes) as a product of the conditional probability distributions of the variables given their parents in the graph:

$$P(X_1, X_2, \dots, X_n) = \prod_{i=1}^{n} P(X_i|Pa(X_i)) \quad (1)$$

where $Pa\ (Xi)$ is the parent set of the variable Xi. For example, considering the BN displayed in Figure 2(a), $P(X1, X2, X3, X4) = P(X1)\ P(X2|X1)\ P(X3|X1, X2)\ P(X4|X2)$.

2.2. Limited memory influence diagram

BN can be extended to a limited memory influence diagram (LIMID) using two additional types of nodes, i.e., decision and utility nodes (Jensen and Nielsen, 2007). In order to visually distinguish decision and utility nodes from chance nodes, decision and utility nodes are conventionally displayed in an influence diagram as rectangles and diamonds, respectively, (Figure 1(b)).

Each decision node consists of a finite set of decision alternatives as its states. A decision node should be assigned as the parent of all those chance nodes whose probability distributions depend on at least one of the decision alternatives (e.g., X_2 in Figure 1(b)). Likewise, the decision node should be the child of all those chance nodes whose states have to be known to the decision maker before making that specific decision (e.g., X_1 in Figure 1(b)).

A utility node express the preferences of the decision maker as to the outcomes of the decision alternatives. Each utility node is attributed to a utility table in which the numbers are not probabilities (unlike CPT) but rather utility values (positive or negative) determined by the decision maker for each configuration of parent nodes, either decision nodes or chance nodes (Jensen and Nielsen, 2007).

For example, considering a set of three mutually exclusive decision alternatives for the node D = {d_1, d_2, d_3} and two states for the node X_3 = $\{x_3^+, x_3^-\}$ in Figure 1(b), the utility table for the node U includes six utility values for combinations of the decision alternatives and the states. Accordingly, the expected utility of the 2nd decision alternative, $EU(d2)$, can be calculated as:

$$EU(d_2) = \sum_{X_3} P(X_3|d_2)\ U(d_2, X_3) = P(x_3^+|d_2)\ U(d_2, x_3^+) + P(x_3^-|d_2)\ U(d_2, x_3^-) \quad (2)$$

As a result, the decision alternative with the maximum expected utility can be selected as the optimal decision, d^*:

$$d^* = \underset{d_i}{argmax}\ EU(d_i) \quad \text{for } i = 1,2,3 \quad (3)$$

Utility values are usually determined according to the preferences of the decision maker. Utility values can also be generated using appropriate utility functions. A utility function should express how much the decision maker prefers one outcome over another outcome, considering his attitude toward the decision problem of interest and respective constraints. In the context of risk-based decision making, utility functions are determined based upon the attitude of the decision maker to risk, which can be risk averse, risk neutral, or risk seeking (Gilboa, 2009).

Application of LIMID in risk-informed decision analysis of chemical and process industries is quite new (CCPS, 2010). To the best of our knowledge, application of LIMID to cost-effective risk management of domino effects is also innovative and unprecedented.

3. Fire protection safety barriers

In this study, both active and passive add-on barriers are analysed. In particular, two types of active barriers are considered: (i) sprinkler systems (SPS), which are typically installed on atmospheric tanks to mitigate the primary fire of the contents of a tank itself or to protect the tank from the fire of a neighbouring tank, and (ii) water deluge systems (WDS), which are typically installed on pressurized vessels (LPG tanks or separators in off-shore plants) to cool the (target) vessels exposed to external fires. Fireproof coating (FPC) is considered as the only passive barrier in the present study.

The evaluation of the performance of the active and passive barriers is schematically depicted in Figure 2, while more details have been presented in Sections 3.1 and 3.2, respectively.

3.1. Active safety barriers

3.1.1. Sprinkler systems

This type of protection, aimed at providing a fire-fighting agent (e.g., water or water-based foam) in order to suppress the primary fire, is typically considered for atmospheric storage tanks for low flash point flammable liquids. Due to process or internal failures, the protection might not respond on demand. Once activated, the barrier is aimed at controlling the primary fire (i.e., reducing the emitting heat radiation) so that the possibility of damage to neighbouring vessels and thus the escalation of the fire can be reduced.

However, even if successfully activated, a non-unitary effectiveness should be considered for the safety barrier as it may fall short to fulfil its desired protection task. Accounting for the probability of failure on demand (PFD) and the effectiveness of the safety barrier (η), the event tree in Figure 2(a) can be used to model the performance of the safety barrier, assuming that an effectively functioning barrier will reduce the emitting heat radiation of the primary fire (Q_o) by 60%, i.e., $Q_e = 0.4\ Q_o$. In the present study, PFD = 5.43×10^{-3} and η = 0.954 (Landucci et al., 2015).

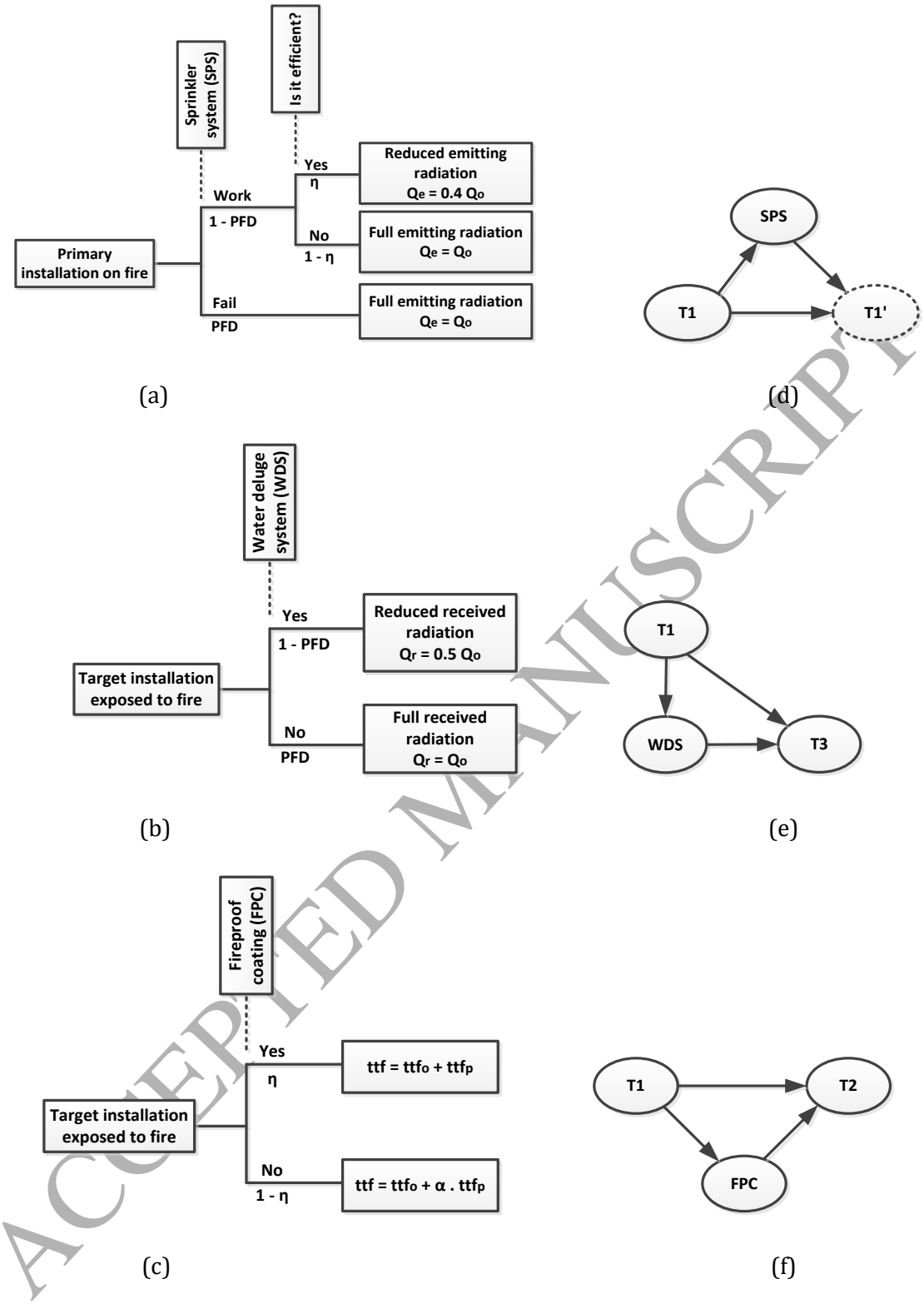

Figure 2. Performance evaluation of the active and passive safety barriers used to protect a target equipment from a primary fire. Using event tree for performance analysis of (a) sprinkler system, (b) water deluge system, and (c) fireproof coating. (d) Using Bayesian network for modelling of (d) sprinkler system (SPS), (e) water deluge system (WDS), and (f) fireproof coating (FPC). Q_0 is the unmitigated heat flux; Q_e is the heat flux mitigated by sprinkler system; Q_r is the heat flux mitigated by water deluge systems; ttf is the time to failure; ttf_0 is the time to failure of target vessel without

fireproofing; ttf_p is the additional time to failure due to the presence of fireproofing coating at maximum efficiency; α is the reduction factor of fireproofing time to failure due to ineffective performance; T1, T2, and T3 are equipment; T1' is an auxiliary node.

3.1.2. Water deluge systems

This type of protection is aimed at providing a spray curtain in order to shield the target vessel from a primary fire. Water deluge systems are applied on target vessels, typically pressurized vessels, and are activated in case of fire. Such as sprinkler systems, due to process or internal failures, this type of safety barriers might not respond on demand, which can be taken into account via a PFD.

If effectively designed and maintained, and successfully activated, the system would completely shield the target vessel, reducing radiation on the wall to a negligible incoming heat flux. However, as demonstrated in previous studies (Finucane and Pinkney, 1988; Roberts, 2004), even if the safety barrier is successfully activated, a fraction of heat radiation can be received by the target vessel in case of inappropriate design or lack of maintenance. In the present study a 50% fraction (i.e., $Q_r = 0.5\ Q_o$) was assumed. This can also be considered as an implicit ineffectiveness of the safety barrier. Accordingly, the event tree in Figure 2(b) can be used to model the performance of water deluge systems, assuming PFD = 4.43×10^{-2} (Landucci et al., 2015).

3.2. Passive safety barriers

The aim of passive fire protection is to increase the time lapse between the start of a primary fire and the eventual failure of the target vessel. This time lapse has been indicated as the time to failure (ttf) of a target vessel (Cozzani et al., 2005; Landucci et al., 2009). In the present work, a straightforward assessment of ttf is instead carried out through the following simplified correlations for vessels without passive protection:

Pressurized vessels: $\ln(ttf) = -0.95 \ln(Q) + 8.85\ V^{0.032}$ (4)

Atmospheric vessels: $\ln(ttf) = -1.13 \ln(Q) - 2.67 \times 10^{-5}\ V + 9.9$ (5)

where ttf is the time to failure (s); Q is the received heat radiation (kW/m^2); V is the target vessel's volume (m^3). Having the ttf, vessel fragility functions (e.g., probit models) can be used to estimate the failure probability of the vessel (Landucci et al., 2009):

$$Y = 9.25 - 1.85 \ln\left(\frac{ttf}{60}\right) \quad (6)$$

$$Pr = \phi(Y - 5) \quad (7)$$

where Y is the probit value; Pr is the failure probability of the target vessel; $\phi(.)$ is the cumulative standard normal distribution. The probit coefficients in Eq. (6) were derived considering a log-normal distribution for the failure probability, under the following assumptions (Landucci et al., 2009):

- 10% probability of failure for ttf = 5 min, which is equal to the time required to start onsite emergency response operations;
- 90% probability of failure for ttf = 30 min, which is equal to the time required to start the mitigation actions.

High performance fireproofing materials, such as intumescent, vermiculite sprays, high performance cementitious materials, and silica blankets, are normally rated to offer a two-hour fire protection with a high efficiency (η = 0.999), even in case of extreme heat radiations (Gomez-Mares et al., 2012). Therefore, the following effectiveness can be assumed:

- η = 0.999, for incoming heat flux < 200 kW/m^2
- η < 0.999, for incoming heat flux > 200 kW/m^2 (not considered in the present study)

Passive fire protections are already in place and do not require external activation; thus, a unitary availability can be considered for such barriers (i.e., PFD = 0). In case of an effective performance, the coating adds an extra time to failure (ttf_p) to the time to failure of the unprotected vessel (ttf_o), thus delaying the failure of the vessel as $ttf = ttf_o + ttf_p$. Ideally, ttf_p = 120 min (rating time), but the coating deteriorates over time due to fire exposure, not maintaining its initial protection integrity (Gomez-Mares et al., 2012). To account for this progressive degradation, in the present study a conservative value of ttf_p = 60 min has been considered, over which the fire resisting properties of the coating were assumed constant.

In case of an ineffective performance, the coating can still extend the ttf_p, yet at a much lower level. Assuming a layer of high performance material with a typically installed thickness of 10mm (Gomez-Mares et al., 2012), if thermal conductivity increases by one order of magnitude (e.g., up to about 1 Wm^{-1}K^{-1}), the protection time will reduce by 75% for severe fire radiation (e.g., about 200 kW/m^2). Thus, for illustrative purposes, in this study a conservative factor α = 1 - 0.75 = 0.25 has been considered to account for ineffective performance of fireproof protection. The event tree in Figure 2(c) can thus be used to model the performance of the passive protection.

Clearly enough, this approach is oversimplified; time-dependent performance of fireproofing should be investigated via appropriate dynamic models to carry out an integrated assessment of the tank and the fireproofing material behaviour during fire exposure (Landucci et al., 2009; Gomez-Mares et al., 2012). The use of tailored models, when available, may constitute an improvement to the current approach in determining the performance of deteriorated and/or damaged fireproof coating materials.

3.3. Safety barrier modelling in Bayesian network

3.3.1. Sprinkler system (SPS)

In order to implement this barrier in BN, the installation and the barrier can be modelled using chance nodes as shown in Figure 2(d) based on the event tree in Figure 2(a). Since this type of barrier is aimed at mitigating the fire at its origin (e.g., a primary tank fire at T1), there should be an arc from the installation (T1 in Figure 2(d)) to the safety barrier (SPS in Figure 1(d)), implying that the latter is triggered by a fire in the former. Accordingly, the mitigation effect of the barrier on the installation, i.e., the mitigated heat radiation, can be articulated in the BN using an auxiliary node (T1' in Figure 2(d)). To account for the performance of the barrier, the conditional probabilities reported in Tables 1 and 2 can be assigned to the barrier and to the auxiliary nodes, respectively.

Table 1. Conditional probability table of SPS in Figure 2(d) given a fire in T1; PFD is the probability of failure on demand of the barrier.

T1	Fire	Safe
SPS		
Fail	PFD	0
Work	1 - PFD	1

Table 2. Conditional probability table of the auxiliary node T1' in Figure 2(d); η is the efficiency of the barrier.

T1	Fire		Safe	
SPS	Fail	Work	Fail	Work
T1'				
Unmitigated heat flux ($Q_e = Q_o$)	1	1 – η	0	0
Mitigated heat flux ($Q_e = 0.4\ Q_o$)	0	η	0	0
Safe ($Q_e = 0$)	0	0	1	1

3.3.2. Water deluge system (WDS)

To implement this barrier in BN, the primary installation, the target installation, and the barrier can be modelled using chance nodes as shown in Figure 2(e). Since this type of barrier is aimed at reducing the heat flux that a target installation receives from an external fire (fire at the primary installation), there should be an arc from the primary installation (T1 in Figure 2(e)) to the safety barrier (WDS in Figure 2(e)), indicating that the latter is activated by the former.

Accordingly, based on whether or not there is a fire in the primary installation and whether or not the barrier is activated, the amount of heat radiation received by the target installation (T3 in Figure 2(e))

and thus its failure probability can be determined. This is why there are arcs from both T1 and WDS to T3 in Figure 2(e). To account for the performance of the barrier, the conditional probabilities reported in Tables 3 and 4 can be assigned to the barrier and the target installation, respectively.

Table 3. Conditional probability table of WDS in Figure 2(e) given a fire in T1; PFD is the probability of failure on demand of the barrier.

T1	Fire	Safe
WDS		
Fail	PFD	0
Work	1 - PFD	1

Table 4. Conditional probability table of T3 in Figure 2(e). P1 and P2 are the failure probabilities given the unmitigated and mitigated heat radiation, respectively, T3 receives from T1.

T1	Fire		Safe	
WDS	Fail	Work	Fail	Work
T3				
Fire	P1	P2	0	0
Safe	1 - P1	1 - P2	1	1

In Table 4, P1 is the failure probability of T3 calculated using Equations (5)-(7) considering the unmitigated heat radiation received from T1 (i.e., $Q_r = Q_o$) due to the failure of WDS; P2 is the one calculated using the mitigated heat radiation received from T1 (i.e., $Q_r = 0.5\ Q_o$) due to the functioning of WDS.

3.3.3. Fireproof coating (FPC)

In order to implement this barrier in BN, the primary installation, the target installation, and the barrier can be modelled using chance nodes in Figure 2(f). As shown in the figure, there is an arc from the primary installation (T1 in Figure 2(f)) to the passive barrier (FPC in Figure 2(f)) and the target installation (T2 in Figure 2(f)) since the barrier is aimed at reducing the heat radiation the target installation receives from the primary installation. Accordingly, based on the state of the primary installation (i.e., "fire" or "safe") and the state of the barrier (i.e., effective or ineffective), the failure probability of the target installation can be determined.

To account for the performance of the barrier, the conditional probabilities can be developed for the passive barrier and the target installation as shown in Tables 5 and 6, respectively. In Table 6, P1 is the

failure probability of the target installation calculated using probit functions, considering ttf = ttf_o + 0.25 ttf_p, while P2 is the one calculated using ttf = ttf_o + ttf_p.

Table 5. Conditional probability table of FPC in Figure 2(f); η is the efficiency of the barrier.

T1	Fire	Safe
FPC		
Ineffective	1 - η	0
Effective	η	1

Table 6. Conditional probability table of the target installation T2 in Figure 2(f). P1 and P2 are the failure probabilities of the target installation given the partial and total protection time ttf_p, respectively.

T1	Fire		Safe	
FPC	Ineffective	Effective	Ineffective	Effective
T2				
Fire	P1	P2	0	0
Safe	1 - P1	1 - P2	1	1

4. Methodology

4.1. An example

In the present study, the BN methodology for domino effect modelling in the chemical industry (Khakzad et al., 2013) was extended to account for the performance of safety measures. For the sake of clarity, the fundamentals of the methodology are demonstrated via a hypothetical chemical storage plant. The characteristics of the plant and allocated safety barriers have been reported in Table 7.

Table 7. Main features of the layout and the safety barriers considered in the demonstrative example.

Layout of the example	ID	Type	Content	V (m^3)	D (m)	H (m)	Allocated fire protection	PFD	η (%)
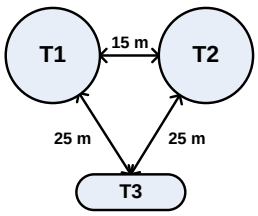	T1	Atmospheric	Benzene	6500	24	14.4	SPS	5.43×10^{-3}	95.4
	T2	Atmospheric	Toluene	6500	24	14.4	SPS , FPC	5.43×10^{-3}, 0.0	95.4, 99.9
	T3	Pressurized	Propane	250	4	18	WDS	4.43×10^{-2}	100

4.2. Domino effect modeling

The escalation modelling is carried out in sequential steps; in the first step, given a primary event, the secondary events are determined, while in the second step the tertiary events are identified, and so on.

- **Step 1**

To model a potential fire escalation in the chemical plant, a node is assigned to each storage tank (T1, T2, and T3 in Figure 3).

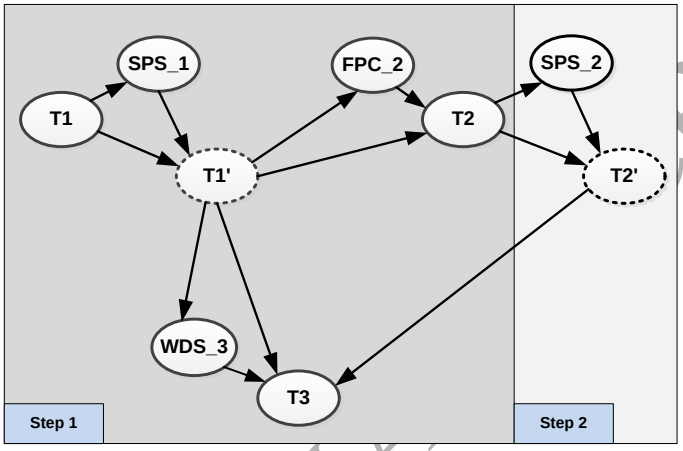

Figure 3. Domino effect modelling using Bayesian network. T1 is the primary event whereas T2 and T3 are the secondary and tertiary events, respectively. The BN has been developed in two steps. The first step, is aimed at identifying the secondary and tertiary events; the second step, is aimed at updating the probability of the tertiary event, taking into account the synergistic effect of the primary and secondary events.

To model the fire propagation through the plant, one of the installations should be identified as the primary unit where a primary fire may initiate the chain of fires. If the aim of the study is the assessment of the worst case domino scenario, the primary unit can be identified via different approaches such as domino indices (Cozzani et al., 2009). Khakzad and Reniers [15] showed that, modelling a chemical plant as a directed graph, a node (process unit) with the highest out-closeness centrality score can lead to the most severe domino effect if selected as the primary installation. In the present example, for illustrative purposes, T1 is specified as the primary unit where a primary tank fire can occur with a probability of 1.0×10^{-4} (FRED, 2012).

Considering a tank fire in T1 as the primary event, the allocated sprinkler system, SPS_1, can be triggered to mitigate the heat radiation emitted from T1. The mitigation effect of SPS_1 on T1 can be modelled via the auxiliary node T1' in Fig. 3. T1' will be used for the rest of the domino effect

modelling as it takes into account both the potential fire in T1 and the mitigation influence of SPS_1. The intensity of the heat radiation originally generated by T1 can be calculated using methodologies described in (CCPS, 2000; Van Den Bosh and Weterings, 2005). In the present study, however, we employed ALOHA software (2014) to calculate the heat radiation of the fire tanks, considering an ambient temperature of 15 °C, 25% relative humidity, and a wind speed of 2 m/s from Northwest. Accordingly, the heat radiation received by T2 and T3 from T1 are calculated as 30 kW/m^2 and 18.5 kW/m^2, respectively. Determining a threshold value of 15 kW/m^2 for heat radiation to cause credible damage (Cozzani et al., 2009), both T2 and T3 can be considered as potential target installations.

Having a fire in T1 (or T1' hereafter), the water deluge system of T3, WDS_3, can be triggered to protect T3 from the input heat radiation. Based on whether the safety barrier operates or fails, the failure probability of T3 can be estimated using the mitigated or unmitigated heat radiation received from T1' by Equations (4), (6), and (7). For example, if T1 is on fire and SPS_1 works effectively, the heat radiation T3 receives from T1' will be mitigated to 0.4 × 18.5 kW/m^2 = 7.4 kW/m^2. This heat radiation can also be lowered to 0.5 × 7.4 kW/m^2 = 3.7 kW/m^2 if WDS_3 works.

Similar to the active safety barrier of T3, the fireproof coating of T2, FPC_2, is aimed at protecting T2 against the heat radiation of T1'. Based on whether FPC_2 is effective or not, the failure probability of T2 can be estimated using the heat radiation received from T1' and via Equations (5)-(7). The account for the impact of T1', arcs have been drawn from T1' to T2, T3, and the safety barriers thereof.

Having the BN developed in Step 1 and the CPTs developed in Section 3.3, the probabilities of fire in T1, T2, and T3 can be calculated using BN software package GeNIe software (2014) as 1.0 × 10^{-4}, 1.13 × 10^{-8}, and 1.60 × 10^{-9}, respectively. Since the failure probability of T2 is higher than that of T3, T2 is considered as the secondary installation being involved in the domino effect.

- **Step 2**

Having a tank fire in T2, as the secondary event, the sprinkler system of T2, SPS_2, can be activated to control the fire and mitigate the heat radiation emitted from T2. Similar to T1, the impact of this barrier on T2 can be modelled via the auxiliary node T2'. To account for the synergistic effect of T1' and T2' on T3, an arc is drawn from T2' to T3.

Using the modified BN, the updated failure probability of T3 as the tertiary event in the domino effect is calculated as 1.62 × 10^{-9}. Thus, the sequence of the events (and their probabilities) in the fire escalation would be T1 (1.0 × 10-^{4}) → T2 (1.13 × 10^{-8}) → T3 (1.62 × 10^{-9}). For the sake of comparison, the sequence of the events (and their probabilities) in the absence of the safety barriers has also been calculated as T1 (1.0 × 10^{-4}) → T2 (8.34 × 10^{-5}) → T3 (7.5 × 10^{-6}).

5. Application of the methodology

5.1. Case study

In this section, an application of the methodology has been demonstrated via a real storage plant comprising ten gasoline (atmospheric) storage tanks as shown in Figure 4(a). Out of the storage tanks, the tanks T1-T4 have a diameter of 50 m and a height of 10 m while the tanks T5-T10 have a diameter of 40m and a height of 10m. The approximate distances among the tanks are shown in Figure 4(b).

In the case study, for the first part of modeling, it is assumed that all the tanks are equipped with sprinkler systems; no other safety barriers are considered. Assuming the same atmospheric conditions as of the example in Section 4, the intensity of heat radiation between each pair of the storage tanks was calculated using ALOHA (2014), assuming tank fire as the most credible accident scenario.

Modeling the storage tanks and the mutual heat radiation vectors as a directed graph, a graph theory approach (Khakzad and Reniers, 2015) can be used to calculate the centrality scores of the tanks (Figure 5). As can be seen, tank T4 indicates the highest out-closeness centrality score. As such, T4 can be identified as the primary unit which may give rise to the most severe domino scenario in the tank farm. The betweenness centrality scores of the tanks have also been displayed in Figure 5, with T3, T4, T5, and T6 as the tanks with the highest betweenness scores. The fireproofing of tanks with the highest betweenness score have been proposed as an effective way to mitigate the propagation of fire (Khakzad and Reniers, 2015).

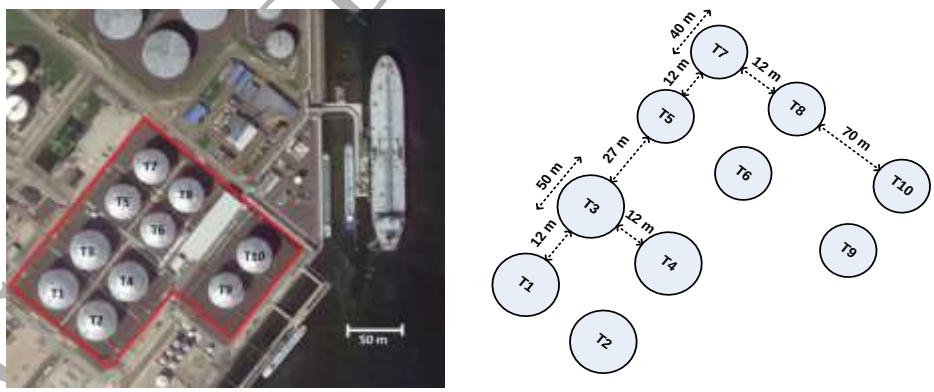

(a) (b)

Figure 4. (a) Storage area comprising ten atmospheric storage tanks. (b) Layout of the plant.

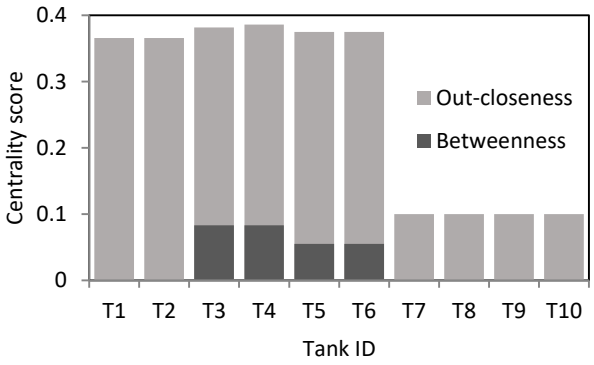

Figure 5. Centrality scores of the storage tanks. Out-closeness and betweenness scores have been indicated using light and dark bars, respectively.

5.2. Fire escalation modelling

Using the methodology developed in Section 4.2, the BN in Figure 6 (denoted by dark-colored nodes) illustrates the escalation of the fire from T4 (1.0×10^{-4}) under the effect of the sprinkler systems in place[1]. Employing the probabilities and effectiveness values previously used in Section 4.2, the failure probabilities of the storage tanks were calculated as reported in the 2nd column of Table 8. Based on the failure probabilities, the expected loss can be estimated as the sum product of tanks' failure probabilities and respective tanks' costs.

Considering the cost of 3.7 M€ and 4.6 M€ for the smaller and larger tanks, respectively (MATCHES), and using the failure probabilities listed on the second column of Table 8, the expected loss would be calculated as 3.06 k€. In the present analysis, for the sake of brevity, only the direct loss of assets (storage tanks) was taken into account in risk assessment, overlooking risks associated with the loss of life, damage to reputation, loss of stored chemicals, and loss of business continuity were not included.

[1] Since the failure of T1, T7, T9, and T10 cannot seem to trigger other accidents, their sprinkler systems and respective auxiliary nodes have been removed from the BN for the sake of simplicity.

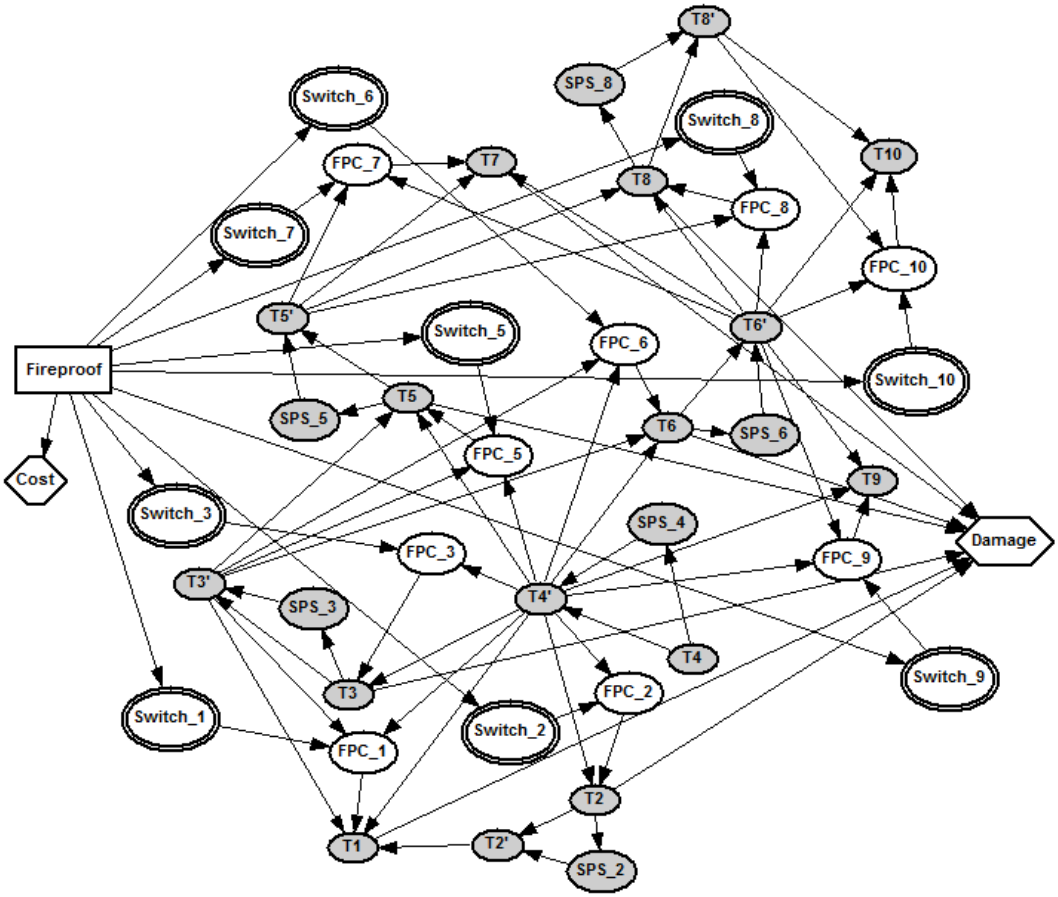

Figure 6. Modeling and risk management of fire domino scenario as a limited memory influence diagram. Sprinkler systems and fireproofing have been indicated as SPS and FPC nodes, respectively.

Table 8. Failure probabilities of the tanks before and after fireproofing plans. The effect of sprinkler systems has been taken into account regardless of fireproofing or not fireproofing of the tanks.

Tank ID	Damage probability (P_i)		
	No fireproofing	T3 is fireproofed	All tanks are fireproofed
T1	9.98E-05	9.79E-05	2.85E-08
T2	9.44E-05	9.44E-05	4.09E-08
T3	9.44E-05	4.09E-08	4.09E-08
T4[a]	1.00E-04	1.00E-04	1.00E-04[a]
T5	8.59E-05	5.03E-05	1.43E-08
T6	8.71E-05	5.38E-05	2.21E-08
T7	8.53E-05	2.98E-05	7.60E-12
T8	8.57E-05	4.14E-05	8.90E-12
T9	1.95E-07	1.91E-07	3.38E-14
T10	1.53E-07	9.44E-08	7.71E-18

[a].T4 is not fireproofed.

5.3. Cost-effective allocation of safety measures

Let's assume that the asset risk of fire escalation in the chemical area has to be decreased via fireproofing of the tanks. For this purpose, the following assumptions are made:

- The amount of budget available for such an additional fire protection is considered as 2.5 M€.
- The unitary cost of fireproofing of a storage tank is 410 € /m^2 (Paltrinieri et al., 2012).

Accordingly, the cost of fireproofing for smaller (the lateral area of 1,884 m^2) and larger (the lateral area of 2,355 m^2) storage tanks is estimated 772 k€ and 966 k€, respectively. Since the fireproofing of the primary tank T4 cannot seem to prevent from the internal causes leading to a tank fire, the total cost of fireproofing for the rest of the tanks comes to 7.53 M€, which is 3 times higher than the allocated budget (2.5 M€). As such, the BN developed in Section 5.2 can be extended to a limited memory influence diagram (by adding the light-colored nodes) to determine which storage tank to fireproof.

The effect of fireproofing is taken into account in the BN by adding the node FPC_i to represent the fireproofing of the tank Ti. Since the available budget is not sufficient to fireproof all the tanks, binary switches (depicted as double outline nodes) have been assigned to each FPC_i to facilitate the inclusion (Switch: on) or exclusion (Switch: off) of the respective fireproofing in different safety allocation strategies. The switches are then manipulated by the decision node, 'Fireproof' in Figure 6, according to the decision alternatives (fireproof strategies) embedded in the decision node. Each decision alternative in the decision node specifies exactly which tanks to fireproof.

For example, consider, among others, the following decision alternatives:

- d-135: the fireproofing of T1, T3, and T5
- d-257: the fireproofing of T2, T5, and T7
- d-16: the fireproofing of T1 and T6.

The table assigned to the deterministic node "Switch_1" in Figure 6 can be represented as Table 9.

Table 9. Table of node "Switch_1" given different fireproofing decision alternatives.

Fireproof	d-135	d-257	d-16
Switch_1			
On	1	0	1
Off	0	1	0

In order to account for the available budget, for the cost of each decision alternative (total cost of fireproofing for the tanks involved in each decision alternative), and for the effectiveness of each

decision alternative (the effect of fireproofing on the total asset risk of the domino effect), the utility nodes "Cost" and "Damage" were added to Figure 6.

Hyperbolic risk aversion utility functions can be used to reflect the risk aversion of a decision maker, implying that the higher the cost of fireproofing (and also the damage to the tanks), the higher risk averted the decision maker. The degree of risk aversion can be expressed, for example, using the coefficient of absolute risk aversion $A(X) = -\frac{U''(X)}{U'(X)}$, where U''(X) and U'(X) are the first and second derivatives of the utility function U(X) with respect to X.

The linear transformation of utility functions, thus, does not change the degree of risk aversion, but introduces a relevant difference in the utility value with respect to, for example, decision criteria or constraints. Therefore, considering the risk aversion of the decision maker towards the cost C of additional safety measures (fireproofing of the storage tanks) and considering an available budget of 2.5 M€, the utility values of the utility node "Cost" in Figure 6 can be determined using the utility function in Equation (8):

$$U(C) = 2.5^2 - C^2 \tag{8}$$

Likewise, the risk aversion of the decision maker toward the cost incurred by the damage of the storage tanks D due to domino effect can be represented using the hyperbolic utility function in Equation (9):

$$U(D) = -100\,D^2 \tag{9}$$

In Equations (8) and (9), both C and D are expressed in million euros.

As can be noted from Equation (8), the total available budget of 2.5 M€ has been accounted for in the utility function so that the fireproofing plans costing more than the budget will be penalized via negative utility values. In case of damage, however, as can be seen from Equation (9), all possible damages are associated with negative utility values. Nevertheless, as in Equation (8), a threshold for the tolerable amount of damage could also have been added as a constant to the utility function in Equation (9).

In the present study, it has been assumed that the two decision criteria cost C and damage D are of the same importance in the selection of an optimal fireproofing strategy. As such, the utility function of the damage in Equation (9) has been multiplied by a factor of 100, so that the expected utility of the damage EU(D) would become of the same order as the expected utility of the cost EU(C).

This is because, for a specific fireproofing strategy, the cost of fireproofing is a certain value (P = 1.0), and thus, the order of the expected utility of cost EU(C) is about U(C). On the other hand, the risk of total damage to the storage plant is an uncertain value ($P \geq 1.0 \times 10^{-4}$), and thus the order of the

expected utility of damage EU(D) would be about $1.0 \times 10^{-4} \times U(D)$. The factor of 100 adopted in Equation (9) can be increased or decreased in order to indicate the higher or lower priority of the damage to the costs, depending on the preference of the decision maker. This factor should be seen as the weight assignment to decision criteria which is undertaken in a wide variety of multi-criteria decision making techniques such as analytic hierarchy process or goal programming (Chvatal, 2002; Saaty, 2008; Gilboa, 2009).

Using the influence diagram developed in Figure 6, the expected utilities of a number of fireproofing plans can be calculated, and the one with the highest expected utility can be determined as the optimal (cost-effective) strategy. To this end, we considered a variety of fireproofing plans, each indicating the number and the identification of the storage tanks to fireproof. Considering 130 plans, as reported in Table 10, the fireproofing of T3 is determined as the optimal fireproofing plan (EU = 2.65), followed by the fireproofing of T5 and T6 (EU = 2.07), and the fireproofing of T3 and T6 (EU = 1.78) as the second and third optimal plans, respectively.

As can be noted from Table 10, all the fireproofing plans referring to more than two storage tanks are attributed to negative expected utilities, mainly due to the budget constraint. Considering the fireproofing of T3 and the fireproofing of all the tanks as the two decision alternatives with the highest and the lowest expected values, respectively, the damage probabilities of the tanks have been reported in the 3rd and 4th columns of Table 8 while the expected loss of assets have been displayed in Figure 7.

Table 10. Fireproofing strategies considered for cost-effectiveness analysis.

Decision alternative description	No. of alternatives	Alternative with the highest expected utility	The value of the highest expected utility
Only one large tank	3	T3	2.65
Two small tanks	15	T5, T6	2.07
One large & one small tanks	18	T3, T6	1.78
Only one small tank	6	T6	1.37
Two large tanks	3	T2, T3	1.21
Two small & one large tanks	45	T5, T6, T1[a]	-0.83
Three small tanks	20	T5, T6, T7	-0.90
Two large & one small tanks	18	T2, T3, T6	-1.59
None of the tanks	1	NA	-0.71
All the tanks	1	NA	-50.46

[a] The decision alternative T5, T6, T3 is also very close, with the expected value of -0.856.

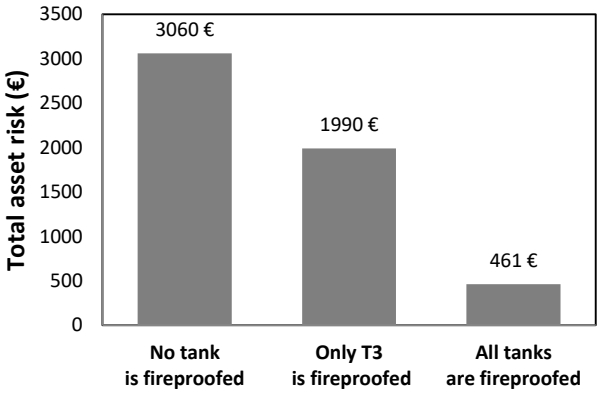

Figure 7. Expected loss of assets before and after fireproofing strategies.

5.4. Discussion

In the previous section, we developed a limited memory influence diagram for modelling and safety management of fire escalation scenarios in chemical plants. Using the developed influence diagram, a number of fireproofing strategies were examined to identify the optimal set of storage tanks to fireproof. The influence diagram can be employed to compare an arbitrarily large number of decision alternatives due to the cardinality characteristic of the utility functions in Equations (8) and (9).

Since cardinal utility functions reflect the levels of absolute satisfaction, the order of preference will not change whether a number of decision alternatives are added or omitted from the decision analysis. This aspect of cardinal utility functions prevents the issue of rank reversal (the change of the order of preference) (Forman, 2001) which is the case with some well-known multi-criteria decision analysis techniques such as analytic hierarchical process (Saaty, 2008). As a result, each time, a manageable set of decision alternatives can be ranked based on the values of their expected utility, and then the one with the highest expected utility can be preserved to be further compared with the next set of decision alternatives. This facilitates the analysis of a large number of fireproofing strategies in order to find the optimal cost-effective strategy.

The number of possible alternatives may drastically increase for more complex configurations of protection systems in larger chemical plants. The protection plans identified in Table 10 were determined based on the available budget, which significantly reduce the number of decision alternatives to consider. According to an available budget of 2.5 M€, a rational decision maker would not consider a fireproofing alternative which may cost 4.0 M€. As such, the number of possible alternatives is always limited.

To reduce the number of alternatives in the case of more complex configurations and plant layouts, it is suggested to perform a simplified preliminary screening in order to i) identify the most critical

targets to protect, and ii) determine the most suitable technology to protect the targets. The former may be carried out via risk-based screening (API-RP 581, 2008; Khakzad and Reniers, 2015) or based on inherent safety principles (Cozzani et al., 2009). The latter is based on industrial standards and best practice indications.

Khakzad and Reniers (2015) illustrated, using a graph theoretic approach, that among the installations of a chemical plant, the ones with the highest betweenness centrality scores contribute the most to the propagation of domino effects; thus, the isolation of such installations (e.g., by means of fireproofing) can significantly reduce the severity and probability of domino effects. As can be seen Figure 5, T3, T4, T5, and T6 have the highest betweenness scores within the chemical plant. Except T4, which also has the highest out-closeness score and thus been identified as the primary unit, the fireproofing of T3, T5, and T6 seems like the most effective (not likely cost-effective) strategy when considering the allocation of extra fire protection. Thus, the outcomes of the influence diagram are in agreement with the results of the graph theoretic approach (Figure 5) since the fireproofing of T3, T5, and T6 (not all together) contribute to most of cost-effective fireproofing strategies in Table 10.

It should be noted that the data used in this study for the failure probability and the effectiveness of safety barriers are generic data adopted from a previous study (Landucci et al., 2015). We employed this generic data merely for illustration purposes; which, otherwise, should be replaced with site-specific data obtained from safety reports or direct inspections, when possible. In the present study, it is assumed that high performance insulation coating (PFD=0; η=0.999) was considered for fireproofing of equipment. This type of coating is normally used in Oil & Gas facilities (Di Padova et al., 2011; Tugnoli et al., 2012). However, fireproof coatings with low performance materials such as glass wool or rock wool can be considered for some facilities due to project time and/or cost constraints (Zuccaro, 2012). Nevertheless, a dedicated approach for the probabilistic assessment of low performance fireproof coatings is still lacking, which will be considered in future studies.

In the present study, the role of emergency response teams, whether internal or external, was not taken into account. The intervention of emergency response teams, aimed at suppression or control of fires, can significantly influence both the severity and the likelihood of fire escalation scenarios. The effectiveness of emergency response actions is largely influenced by several time elements, including time to detection, time to alert, time to deployment, and time to final mitigation (Landucci et al., 2015). This dynamic nature of emergency response actions demands for dynamic tools, such as dynamic Bayesian network (Khakzad, 2015) or dynamic event sequence diagram (Zhou et al., 2016), which is beyond the scope of the present study but will be pursued in the near future.

Domino scenarios in chemical and process plants are among high-impact low-frequency (HILP) events, which are barely taken into account in plants' risk assessment and management. For those plants which account for the impact of domino effects, the common practice is to consider the worst-case

domino effect, in terms of likelihood and severity. Khakzad and Reniers (2015) illustrated that a fire or explosion at a process vessel with the highest out-closeness score can result in the most severe domino scenario in the plant. As described in Section 5.1, the selection of the primary unit in the present study has been based on the calculated out-closeness scores in Figure 5.

It, however, should be noted that forcing the BN to model a domino scenario from a specific unit (node) may not present the most accurate picture of the event. Khakzad (2015) developed a methodology based on dynamic BN to consider all domino scenarios that may occur in a chemical plant without forcing the model to initiate the domino effect from a specific primary unit. Nevertheless, we purposely chose a conventional BN over dynamic BN to keep the study's focus on the modelling of safety measures in BN and their effect on fire propagation. A similar implementation of safety measures can be performed in a dynamic BN framework which not only considers all possible domino scenarios but also account for temporal degradation of safety measures.

6. Conclusions

In the present study, a methodology based on Bayesian network was developed for modeling fire escalation during domino effects while accounting for the impact (availability and effectiveness) of fire protection safety measures. The Bayesian network was converted to an influence diagram to identify most cost-effective allocation of extra safety measures where further prevention and mitigation was required. The comparison of the results obtained from the influence diagram with the results of previous study based on the application of graph theory demonstrated the efficacy and reliability of the developed methodology. The developed methodology can be of great application in large chemical plants where due to the presence of many decision parameters (e.g., available budget, cost of safety barriers, failure probability and efficiency of safety barriers, etc.) and decision alternatives (e.g., which safety barrier should be allocated to which installation) the application of other multi criteria decision analysis techniques such as AHP is limited.

References

Abdolhamidzadeh B, Abbasi T, Rashtchian D, Abbasi SA. A new method for assessing domino effect in chemical process industry. Journal of Hazardous Materials, 2010; 182: 416–26.

ALOHA, 2014. US Environmental Protection Agency, National Oceanic and Atmospheric Administration. Available at: <http://www.epa.gov/OEM/cameo/aloha.htm> (accessed on 1 May 2016).

Arturson G. The tragedy of San Juanico - the most severe LPG disaster in history. Burns Including Thermal Injury, 1987; 13(2): 87–102.

American Petroleum Institute. API-RP 581. Risk-based inspection technology. 2nd Edition, September 2008. Washington, D.C., US. Available online from: http://www.irantpm.ir/wp-content/uploads/2011/08/API-581-2008.pdf.

Bagster, DF, Pitblado, RM. The estimation of domino incident frequencies - An approach. Process Safety and Environmental Protection 1991; 69: 195–199.

BBC. 2010. How the Buncefield fire happened. http://www.bbc.com/news/uk-10266706

Bernechea E, Arnaldos J. Optimizing the design of storage facilities through the application of ISD and QRA. Process Safety and Environmental Protection 2014; 92, 598–615.

CCPS. Guidelines for Chemical Process Quantitative Risk Analysis, 2nd ed.New York: AIChE, 2000.

CCPS. Tools for Making Acute Risk Decisions: With Chemical Process Safety Applications. New York: AIChE, 2010.

Chvatal V. 1983. Linear programming. New York: W.H. Freeman & Co Ltd., ISBN: 978-0716711957.

Cozzani V, Gubinelli G, Antonioni G, Spadoni G & Zanelli S. The assessment of risk caused by domino effect in quantitative area risk analysis. Journal of Hazardous Materials 2005; A127: 14–30.

Cozzani V, Tugnoli A & Salzano E. The development of an inherent safety approach to the prevention of domino effects. Accidents Analysis and Prevention 2009; 41: 1216–1227.

Council Directive 2012/18/EU. European Parliament and Council Directive of 4 July 2012 on control of major-accident hazards involving dangerous substances. Official Journal of the European Communities,2012, L197/1.

Darbra RM, Palacios A, Casal J. Domino effect in chemical accidents: Main features and accident sequences. Journal of Hazardous Materials, 2010; 183: 565–573.

Di Padova A, Tugnoli A, Cozzani V, Barbaresi T, Tallone F. Identification of fireproofing zones in Oil&Gas facilities by a risk-based procedure. Journal of Hazardous Materials 2011; 191, 83–93.

Finucane M, Pinkney D. 1988. Reliability of Fire Protection and Detection Systems, SRD R431. Edinburgh (UK): United Kingdom Atomic Energy Authority, University of Edinburgh.

Forman EH, Saul IG. The analytical hierarchy process-an exposition. Operations Research 2001; 49 (4): 469–487.

FRED (2012). Failure Rate and Event Data for use within Risk Assessments, HSE 2012.

GeNIe, 2014. Decision Systems Laboratory, University of Pittsburgh. Available online at: http://www.bayesfusion.com.

Gilboa I. 2009. Theory of Decision under Uncertainty. Cambridge University Press, New York, USA, ISBN 978-0-521-51732-4.

Gledhill J, Lines I. Development of Methods to Assess the Significance of Domino Effects from Major Hazard Sites. CR Report 183, Sudbury, UK: Health and Safety Executive, 1998.

Gomez-Mares M, Tugnoli A, Landucci G, Cozzani V. Performance Assessment of Passive Fire Protection Materials. Industrial & Engineering Chemistry Research 2012; 51(22): 7679–7689.

Jensen FV, Nielsen TD. 2007. Bayesian Networks and Decision Graphs, second ed. Springer, New York.

Khan F, Abbasi SA. Models for domino analysis in chemical process industries. Process Safety Progress 1998; 17: 107–123.

Khan FI, Abbasi SA. The world's worst industrial accident of the 1990s: What happened and what might have been - A quantitative study. Process Safety Progress, 1999; 18: 135–145.

Khakzad N, Khan F, Amyotte P, Cozzani V. Domino effect analysis using Bayesian networks. Risk Analysis 2013; 33(2): 292-306.

Khakzad N. Application of dynamic Bayesian network to risk analysis of domino effects in chemical infrastructures. Reliability Engineering and System Safety 2015; 138: 263–272.

Khakzad N, Reniers G. Using graph theory to analyse the vulnerability of process plants in the context of cascading effects. Reliability Engineering & System Safety 2015; 143: 63-73.

Landucci G, Gubinelli G, Antonioni G, Cozzani V. The assessment of the damage probability of storage tanks in domino events. Accident Analysis and Prevention 2009; 41: 1206–15.

Landucci G, Argenti F, Tugnoli A, Cozzani V. Quantitative assessment of safety barrier performance in the prevention of domino scenarios triggered by fire. Reliability Engineering & System Safety 2015; 143: 30-43.

MATCHES. Available online at http://www.matche.com/equipcost/Tank.html.

Nguyen QB, Mebarki A, Ami Saada R, Reimeringer M. Integrated probabilistic framework for domino effect and risk analysis. Journal of Advances in Engineering Software, 2009; 40: 892–901.

Paltrinieri N, Bonvicini S, Spadoni G, Cozzani V. Cost-benefit analysis of passive fire protections in road LPG transportation. Risk Analysis 2012; 32: 200–19.

Pearl J. 1988. Probabilistic Reasoning in Intelligent Systems. Morgan Kaufmann, San Francisco, CA.

Reniers GLL, Dullaert W, Ale BJM, Soudan K. The use of current risk analysis tools evaluated towards preventing external domino accidents. Journal of Loss Prevention in Pro-cess Industries, 2005; 18:119–126.

Roberts TA. Directed deluge system designs and de-termination of the effectiveness of the currently recommended minimum deluge rate for the protection of LPG tanks. Journal of Loss Prevention in the Process Industries 2004; 17: 103–109.

Saaty T. 2008. Decision Making for Leaders: The Analytic Hierarchy Process for Decisions in a Complex World. RWS Publications, Pittsburgh, Pennsylvania, ISBN 0-9620317-8-X.

Tugnoli A, Cozzani V, Di Padova A, Barbaresi T, Tallone F. Mitigation of fire damage and escalation by fireproofing: a risk-based strategy. Reliability Engineering and System Safety 2012; 105, 25–35.

U.S. Chemical Safety Board (CSB). 2015. Caribbean Petroleum Refining Tank Explosion and Fire. http://www.csb.gov/caribbean-petroleum-refining-tank-explosion-and-fire.

Van Den Bosh CJH & Weterings RAPM. 2005. Methods for the calculation of physical effects (Yellow Book), 3rd ed. The Hague (The Netherlands): Committee for the Prevention of Disasters.

Vilchez AJ, Montiel H, Casal J. Arnaldos J. Analytical expressions for the calculation of damage percentage using the probit methodology. Journal of Loss Prevention in the Process Industries, 2001; 14: 193–197.

Zhou J, Reniers G, Khakzad N. Application of event sequence diagram to evaluate emergency response actions during fire-induced domino effects. Reliability Engineering and System Safety 2016; 150: 202–209.

Zuccaro G. 2012. A case of choice of passive fire protection (PFP) in an oil & gas EPC project. Chemical Engineering Transactions. 26, 315–320.